Supporting Information for

Noble-Metal-Free Metal Hydroxide Co-Catalyst Coupled Mn(II)-Doped CdS Nanorods with Bridged Charge Transport for Enhanced Photocatalytic Hydrogen Generation

Walker MacSwain,[b] Xia Hu,†[a] Rongzhen Wu,[c] Zhi-Jun Li,[b] Vanshika Vanshika,[b] De-Kun Ma,[d] Ou Chen,[c] Weiwei Zheng[b]†

[a]†School of Life and Environmental Sciences, Shaoxing University, Shaoxing, 312000, P. R. China
[b]† Department of Chemistry, Syracuse University, Syracuse 13244, New York, USA
[c] Department of Chemistry, Brown University, Providence 02912, Rhode Island, USA
[d] Zhejiang Key Laboratory of Functional ionic membrane Materials and Technology for Hydrogen Production, Shaoxing University, Shaoxing 312000, China

Table of Contents

I. Experimental Details of Control Experiments

Chemicals. Zinc diethyldithiocarbamate ($Zn(DDTC)_2$, 98% Sigma-Aldrich), oleylamine (OAm, 70%, Sigma-Aldrich), 1-octadecene (ODE, 90%, Alfa-Aesar), oleic acid (OA, 90%, Sigma-Aldrich), ethyl acetate (≥99%, ACROS), hexane (99%, EMD), nickel nitrate hexahydrate (99.9985%, STREM), cobalt nitrate hexahydrate (99%, Thermo-Fisher), ferric nitrate nonahydrate (98.5%, Fisher-Scientific), and ethanol (≥99%, anhydrous, Pharmco). Deionized water was used in all experiments. All chemicals were used as purchased without further purification.

A. Synthesis of 1D Mn:CdS/ZnS core/shell NRs. Core/shell NRs were synthesized according to a slightly modified literature procedure.[1, 2] Typically, the as-purified 1D Mn:CdS NRs were dissolved in 9 mL ODE and 3 mL OAm. After that 228 mg (0.63 mmol) of $Zn(DDTC)_2$ was added to the NR (0.45 mmol) solution in a three-neck flask and was vacuumed from room temperature to 80°C and kept vacuuming at 80°C for additional 1.5 hours. Under Ar flow, the reaction solution was heated to a target growth temperature at 220 °C for 1.5 hours. At the end of the reaction, the solution was removed from the heating mantle and allowed to cool to approximately 60 °C. The core/shell NRs were separated from the crude solution by precipitating the particles with ethanol and centrifuging. The precipitate was further purified once by resuspending the NRs in hexane and then reprecipitating with ethanol and centrifugation.

B. Synthesis of 1D Mn:CdS/ZnS-Ni(OH)$_2$ and CdS-Ni(OH)$_2$ NRs. The 1D Mn:CdS/ZnS-$Ni(OH)_2$ hybrid photocatalysts were synthesized according to a literature method.[3] First, 0.23 mmol of the ligand exchanged, water soluble Mn:CdS/ZnS NRs or CdS NRs were dispersed in 5 mL of 0.05 M NaOH aqueous solution, and then a certain volume of 0.05 M $Ni(NO_3)_2$ aqueous solution (typically, 1.1 mL, 0.055 mmol; molar ratio between CdS:$Ni(OH)_2$ 1:0.23) was added dropwise under stirring. The resulting mixture was stirred for a certain amount of time at room temperature (typically one hour). After that, the precipitate was washed three times with deionized methanol and ethyl acetate.

C. Synthesis of 1D CdS-Co(OH)$_2$ NRs. The synthesis of 1D CdS-$Co(OH)_2$ hybrid photocatalysts followed the previously mentioned method[4] except the 0.05 M $Ni(NO_3)_2$ aqueous solution is replaced with 0.05 M $Co(NO_3)_2$ aqueous solution, the typical reaction time is raised to three hours, and the typical molar ratio is raised to (1:0.25).

D. Synthesis of hybrid 1D CdS-Fe(OH)$_3$ NRs. The synthesis of 1D CdS-$Fe(OH)_3$ hybrid photocatalysts followed the previously mentioned method except the 0.05 M $Ni(NO_3)_2$ aqueous solution is replaced with 0.05 M $Fe(NO_3)_3$ aqueous solution, the typical reaction time is two hours, and the typical molar ratio is changed to (1:0.35).

II. Characterization of 1D CdS-based NRs

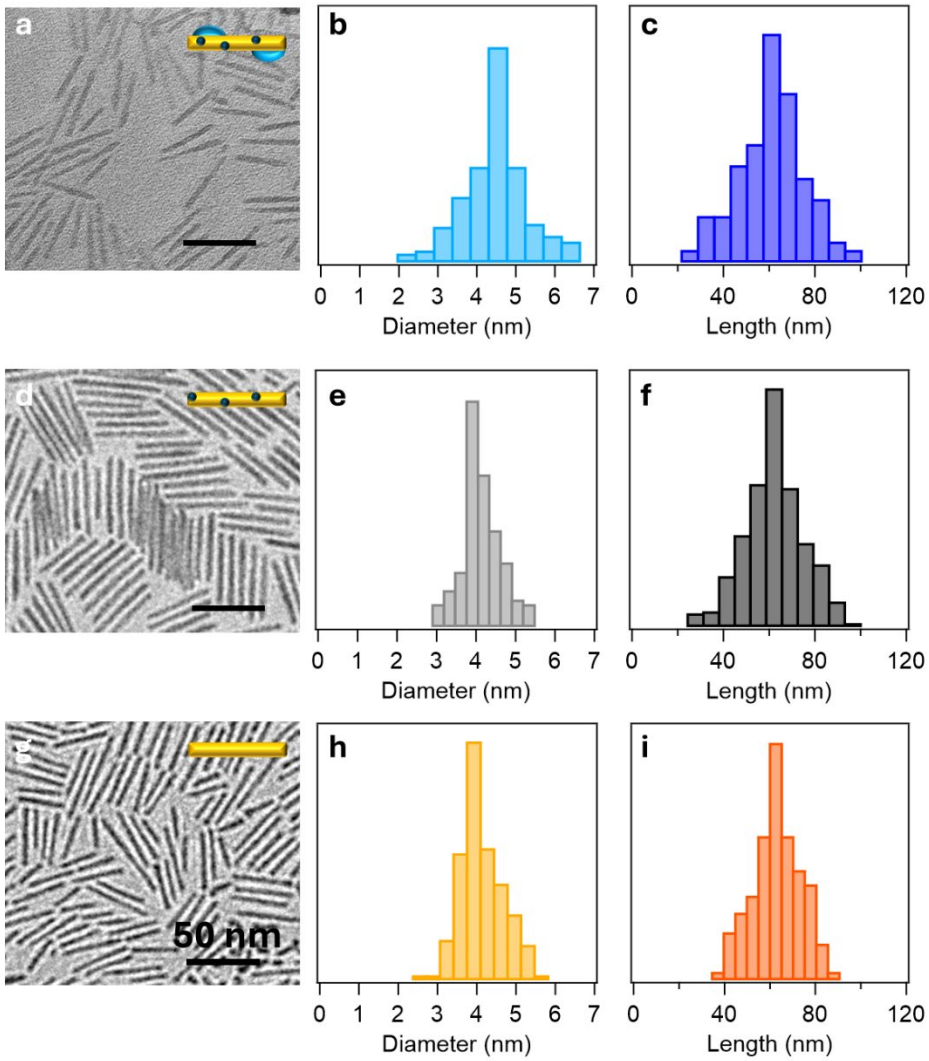

Figure S1. TEM images of a) Mn:CdS-Ni$(OH)_2$, d) Mn:CdS, and g) CdS NRs. Histograms of the diameter for b) Mn:CdS-Ni$(OH)_2$, e) Mn:CdS, and h) CdS NRs and histograms of the length of c) Mn:CdS-Ni$(OH)_2$, f) Mn:CdS, and i) CdS NRs.

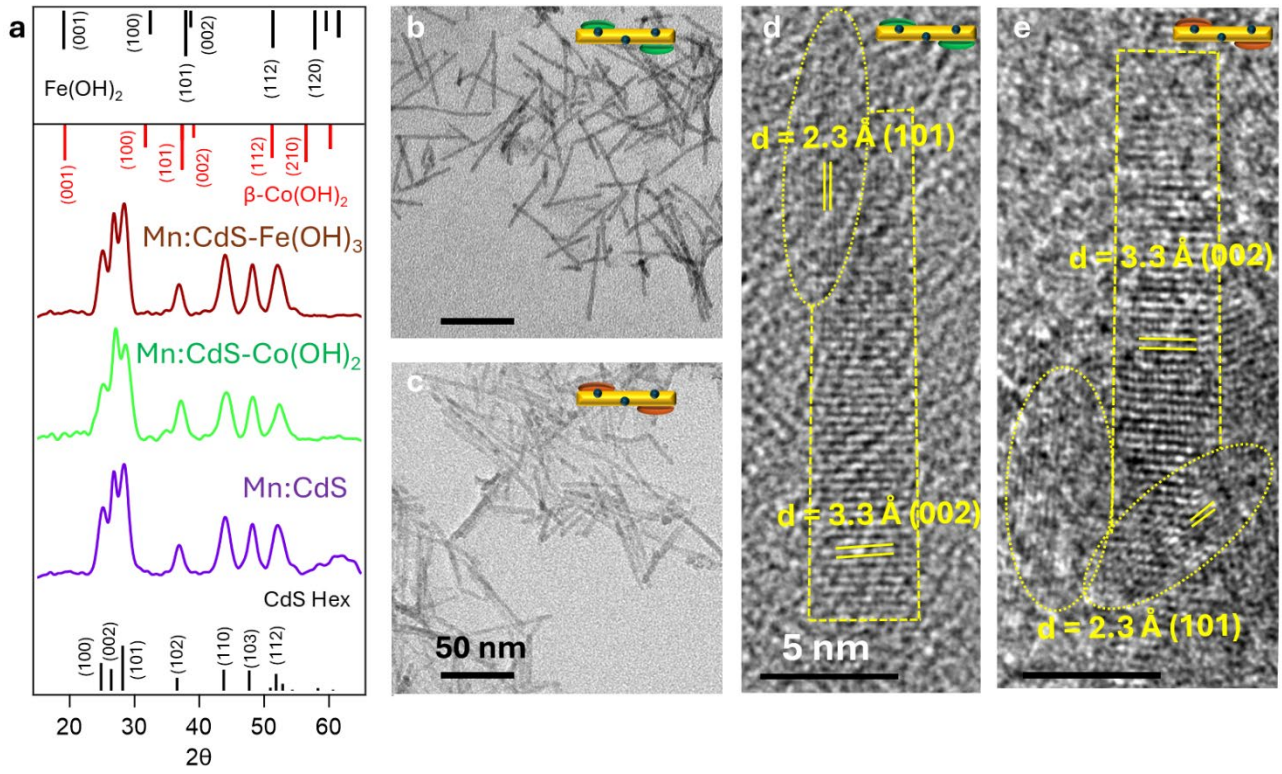

Figure S2. Structural and morphology characterization of Mn:CdS $M(OH)_x$ (M = Co^{2+} and Fe^{3+}) decorated NRs by a) XRD with pure $M(OH)_x$ (M = Co^{2+} and Fe^{3+}) XRD patterns. b and c) TEM characterization, and d and e) HR-TEM characterization. Green samples are the $Co(OH)_2$ while brown samples are the $Fe(OH)_3$ samples, respectively in the TEM and HR-TEM.

Table S1. Molar Ratio between the $M(OH)_x$ and the 1D NRs (*i.e.,* molar ratio between CdS/$Ni(OH)_2$ 1/0.11) as-calculated from ICP-OES measurements.

Sample	Molar Ratio (Metal/Cd)
Mn:CdS-$Ni(OH)_2$	0.11
Mn:CdS-$Co(OH)_2$	0.12
Mn:CdS-$Fe(OH)_3$	0.16

Table S2. As-calculated lifetimes (< τ>) of the NR photocatalysts from PL lifetime.

Sample	< τ> (ns)
CdS	5.6
Mn:CdS	4.9
CdS-$Ni(OH)_2$	3.6
Mn:CdS-$Ni(OH)_2$	1.9
CdS-$Co(OH)_2$	4.2
Mn:CdS-$Co(OH)_2$	2.6
CdS-$Fe(OH)_3$	4.3
Mn:CdS-$Fe(OH)_3$	2.8
Mn:CdS/ZnS	3.0
Mn:CdS-ZnS-$Ni(OH)_2$	1.6

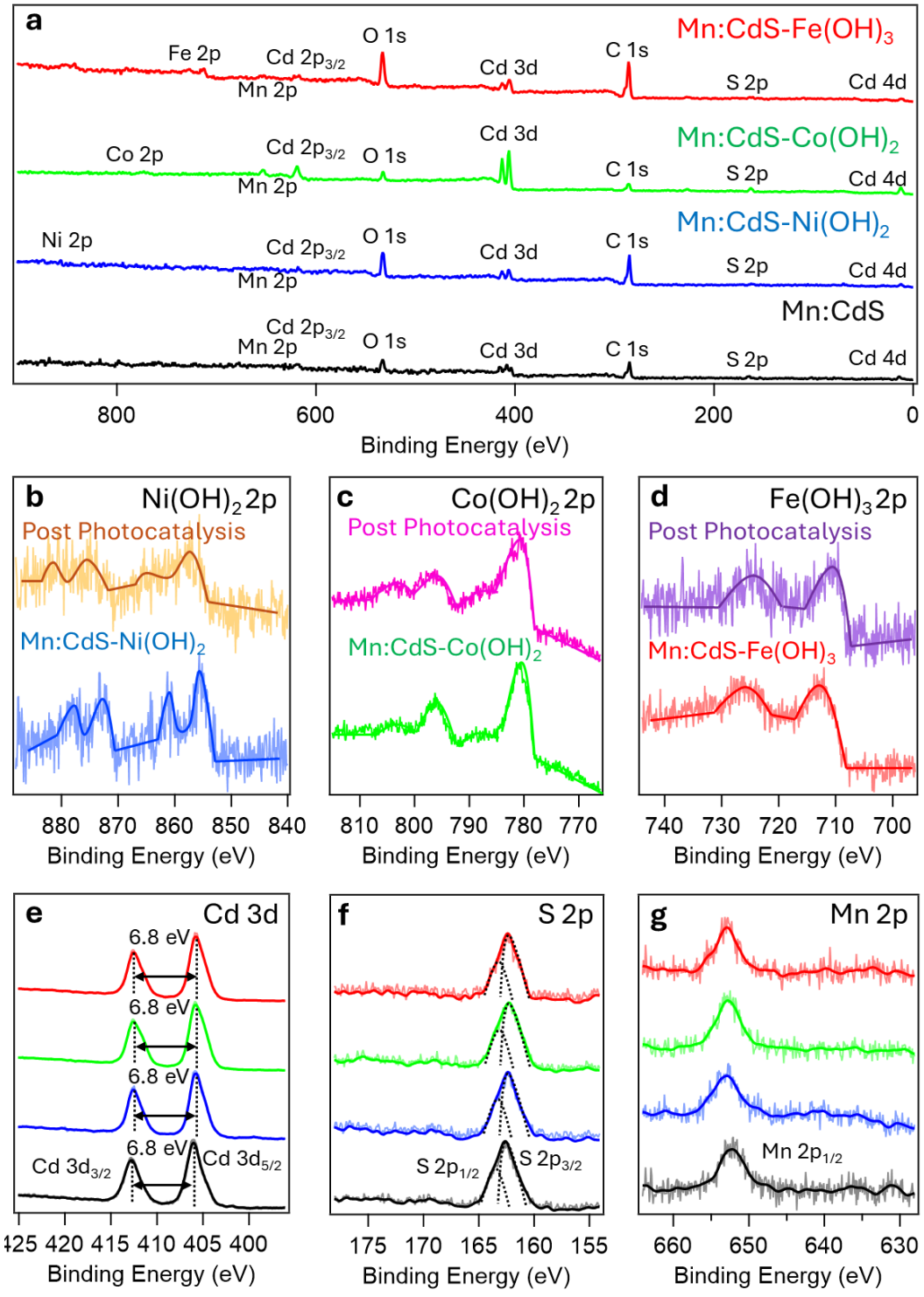

Figure S3. Absorbance X-ray photoelectron spectroscopy (XPS) of 1D Mn:CdS (black), Mn:CdS-$Ni(OH)_2$ (blue), Mn:CdS-$Co(OH)_2$ (green), and Mn:CdS-$Fe(OH)_3$ (red), where (a) is the survey spectrum; b, c, and d) are the Ni 2p, Co 2p, and Fe 2p orbitals before and after photocatalysis for Mn:CdS-$Ni(OH)_2$, Mn:CdS-$Co(OH)_2$, and Mn:CdS-$Fe(OH)_3$, respectively; e) is the Cd 3d orbitals; f) is the S 2p orbitals;, and g) is the Mn 2p orbitals for each sample.

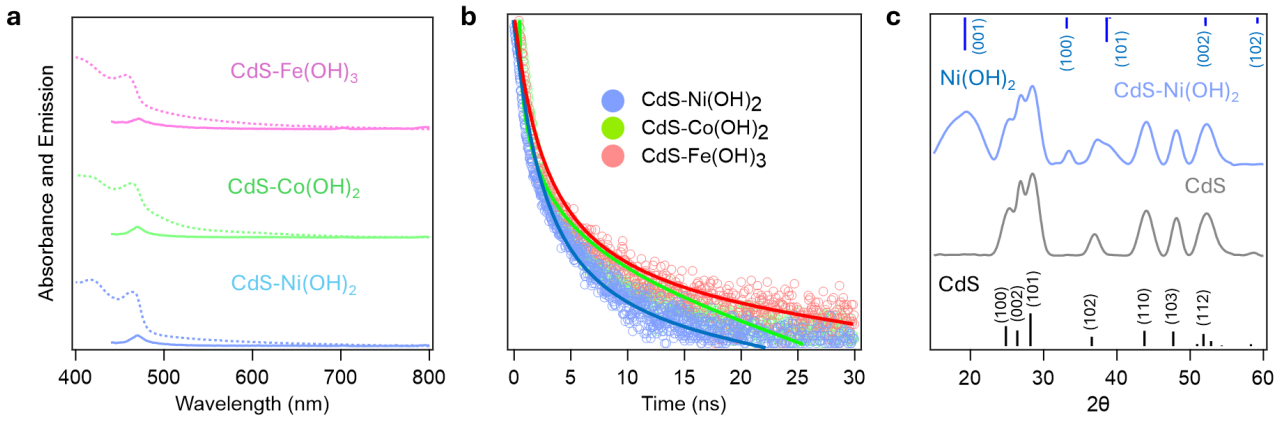

Figure S4. a) Absorbance, PL, and b) PL lifetime data of CdS-M(OH)$_x$ (M = Ni^{2+}, Co^{2+}, and Fe^{3+}) NRs. c) XRD structural and morphology characterization of the CdS-Ni(OH)$_2$ NRs. Reference XRD patterns for Ni(OH)$_2$ is COD 1011134, while CdS is JCPDS 6-314.

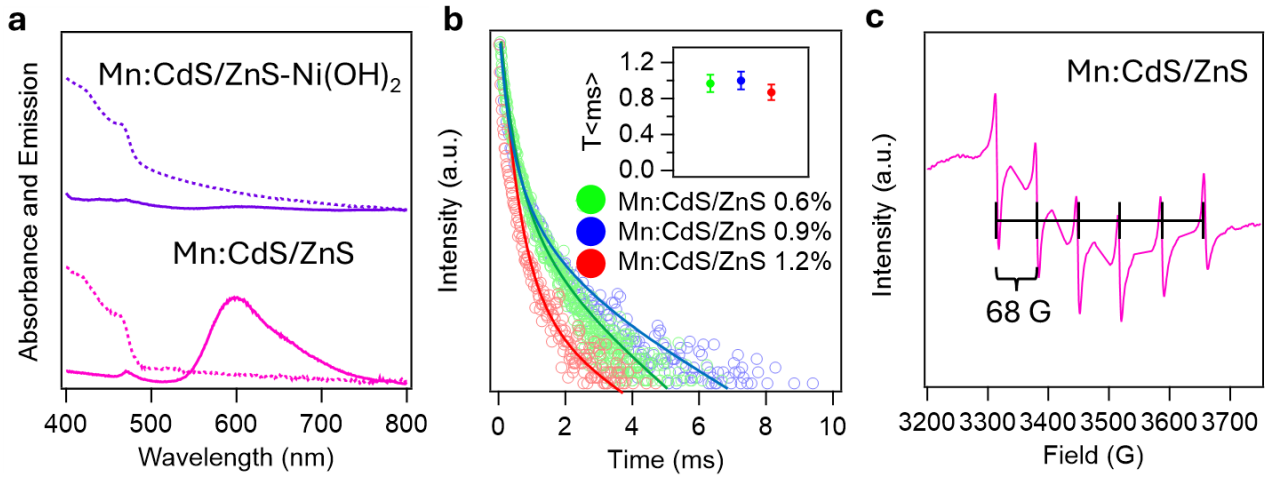

Figure S5. a) Absorbance and PL of Mn:CdS/ZnS and Mn:CdS/ZnS-Ni(OH)$_2$ NRs. b) PL lifetime data with inset calculated lifetimes of core/shell NRs Mn:CdS/ZnS with differing [Mn] dopants. c) EPR measurements of the core/shell Mn:CdS/ZnS NRs.

III. Electrochemical Measurements.

Table S3. As-calculated R_s and R_{ct} (< τ>) of the NR photocatalysts from EIS fits.

Sample	R_s (Ω)	R_{ct} (Ω)
CdS	131.2	2670
Mn:CdS	86.4	1082
CdS-$Ni(OH)_2$	69.4	215.8
Mn:CdS-$Ni(OH)_2$	36.1	133.9
CdS-$Co(OH)_2$	84.2	252.3
Mn:CdS-$Co(OH)_2$	41.3	142.3
CdS-$Fe(OH)_3$	91.1	281.3
Mn:CdS-$Fe(OH)_3$	43.2	151.9

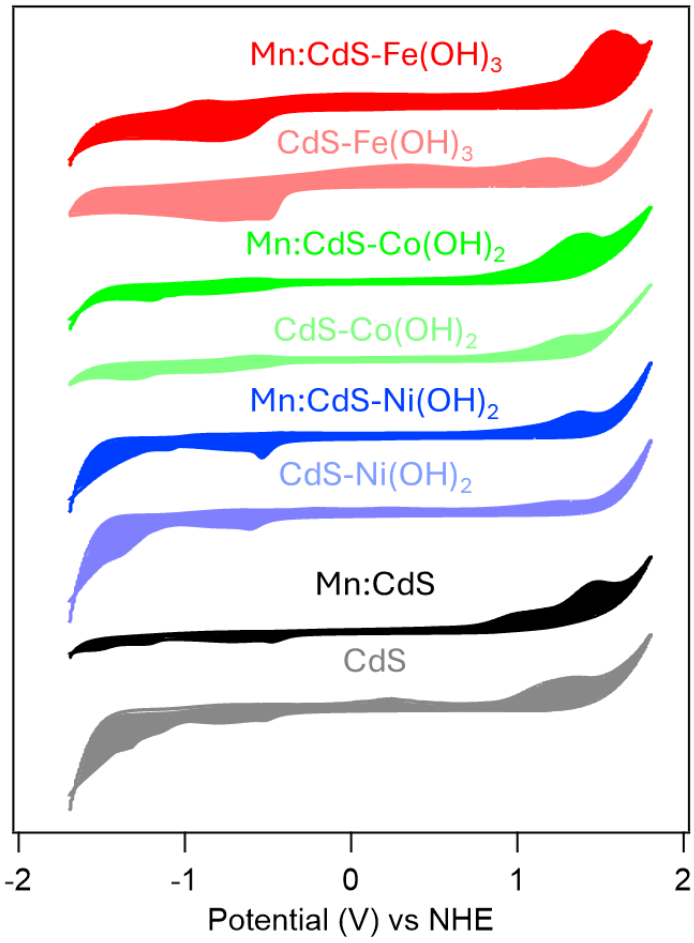

Figure S6. CV of CdS, Mn:CdS, and their corresponding $M(OH)_x$ (M = Ni^{2+}, Co^{2+}, and Fe^{3+}) NRs.

IV. Photocatalytic Water Splitting Studies

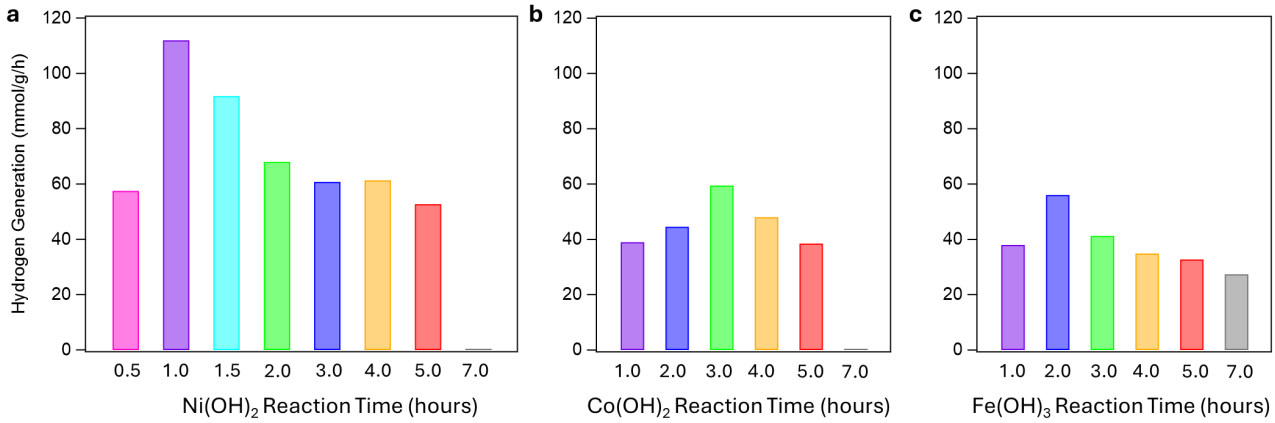

Figure S7. $M(OH)_x$ (M = a) Ni^{2+}, b) Co^{2+}, and c) Fe^{3+}) co-catalyst reaction time dependent photocatalysis.

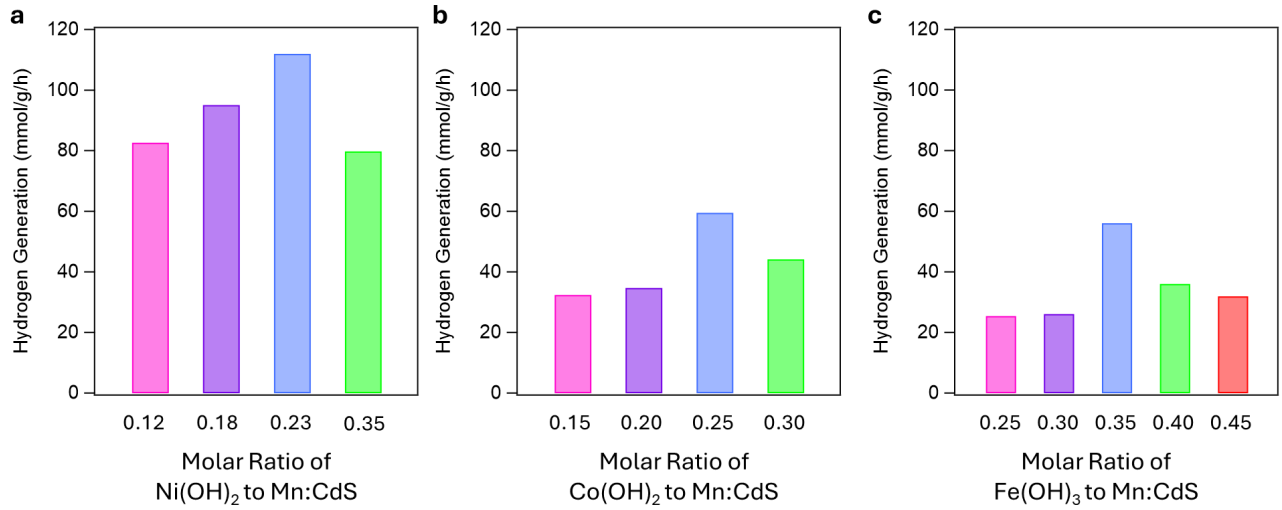

Figure S8. $M(OH)_x$ (M = a) Ni^{2+}, b) Co^{2+}, and c) co-catalyst loading concentration dependent photocatalysis.

V. Internal Quantum Efficiency (IQE) Calculations

The IQE measurements were carried out under simulated solar irradiation (AM1.5G, 100 mW/cm^2, Newport 91160) using a solar simulator illuminating a 4.8 cm^2 reactor area under striring at 1000 rpm. The volume of the generated H_2 gas was collected in a burette and recorded every 15 minutes. For example, the Mn:CdS NRs generated 6.8 mL under solar simulated irradiation for 1 hr. Internal quantum efficiency can be defined as the ratio between the charge utilization of a photocatalytic system divided by the number of photons that reach the cell's surface.[5] The relationship of quantum efficiency to photocatalytic water splitting is defined in equation 1 and 2.

$$QE(\%) = \frac{reacted\ electrons}{incident\ photons} \times 100\% \quad (Eq.\ 1)$$

$$QE(\%) = \frac{\#\ of\ H_2\ molecules \times 2}{incident\ photons} \times 100\%\ (Eq.\ 2)$$

The QE ratio can mathematically be described then by equation 3 where the ΔG^0 (J mol^{-1}) as the standard Gibbs free energy for the formation of H_2 molecules, R (mol s^{-1}) as the rate of generation of H_2 molecules, E_s (J s^{-1} m^{-2}) as the incident photons, and A (m^2) as the irradiated area of the photochemical system.[6]

$$QE(\%) = \frac{\Delta G^0 R}{E_s A} \times 100\%\ (Eq.\ 3)$$

ΔG can be obtained from the Equation 4 below, which is the Nernst equation where n is the number of electrons transferred in the reaction, F (C mol^{-1}) is Faraday's constant, and E (V) is the potential difference.

$$\Delta G = -nFE\ (Eq.4)$$

Finally, the IQE can be calculated by combining equations 2-4, given that the potential of photocatalytic water splitting is 1.23 V, the photocatalytic system has 0.151 W/cm^2 of photon irradiation of which the CdS based NRs can only absorb ~20% of the total irradiation (Figure 2a in the main manuscript), the area irradiated is 4.8 cm^2, and the rate can be calculated by converting the moles of hydrogen generated into a rate of mol per second. The as calculated internal quantum efficiencies are given in Figure S9 below.

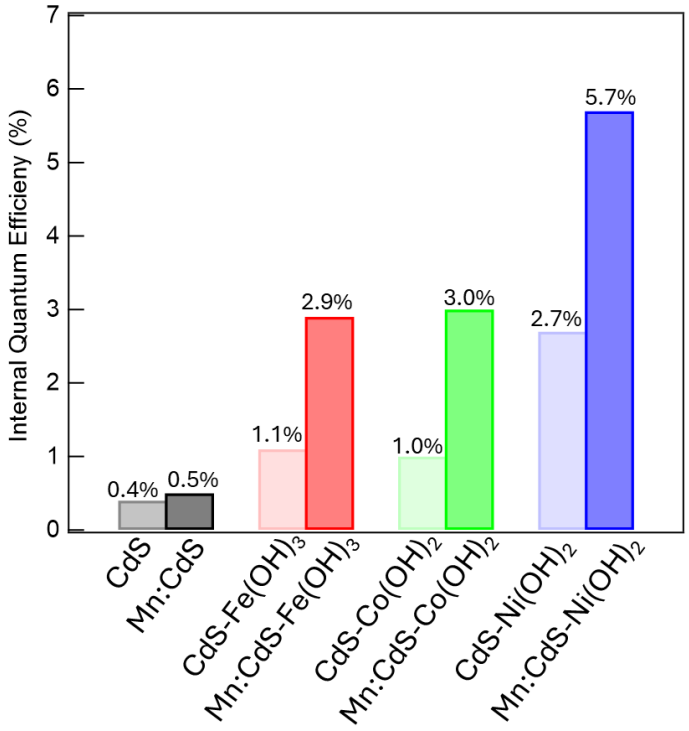

Figure S9. The experimentally measured internal quantum efficiencies of CdS, Mn:CdS, CdS-$Fe(OH)_3$, Mn:CdS-$Fe(OH)_3$, CdS-$Co(OH)_2$, Mn:CdS-$Co(OH)_2$, CdS-$Ni(OH)_2$, and Mn:CdS-$Ni(OH)_2$. The internal quantum efficiencies were measured at pH = 7 for CdS, Mn:CdS, CdS-$Ni(OH)_2$, and Mn:CdS-$Ni(OH)_2$ and at pH > 12 for CdS-$Fe(OH)_3$, Mn:CdS-$Fe(OH)_3$, CdS-$Co(OH)_2$, and Mn:CdS-$Co(OH)_2$ to show the maximum values.

References.

1. Hofman, E.; Khammang, A.; Wright, J. T.; Li, Z.-J.; McLaughlin, P. F.; Davis, A. H.; Franck, J. M.; Chakraborty, A.; Meulenberg, R. W.; Zheng, W. Decoupling and Coupling of the Host–Dopant Interaction by Manipulating Dopant Movement in Core/Shell Quantum Dots. *J. Phys. Chem. Lett.* **2020**, 11, (15), 5992-5999.

2. Davis, A. H.; Hofman, E.; Chen, K.; Li, Z.-J.; Khammang, A.; Zamani, H.; Franck, J. M.; Maye, M. M.; Meulenberg, R. W.; Zheng, W. Exciton Energy Shifts and Tunable Dopant Emission in Manganese-Doped Two-Dimensional CdS/ZnS Core/Shell Nanoplatelets. *Chem. Mater.* **2019**, 31, (7), 2516-2523.

3. Ran, J.; Yu, J.; Jaroniec, M. $Ni(OH)_2$ modified CdS nanorods for highly efficient visible-light-driven photocatalytic H2 generation. *Green Chem.* **2011**, 13, (10), 2708.

4. Zhou, X.; Jin, J.; Zhu, X.; Huang, J.; Yu, J.; Wong, W.-Y.; Wong, W.-K. New $Co(OH)_2$/CdS nanowires for efficient visible light photocatalytic hydrogen production. *J. Mater. Chem. A* **2016**, 4, (14), 5282-5287.

5. Zhang, J.; Yu, J.; Jaroniec, M.; Gong, J. R. Noble Metal-Free Reduced Graphene Oxide-$Zn_xCd_{1-x}S$ Nanocomposite with Enhanced Solar Photocatalytic H_2-Production Performance. *Nano Lett.* **2012**, 12, (9), 4584-4589.

6. Murugan, A. V.; Muraliganth, T.; Manthiram, A. Rapid, Facile Microwave-Solvothermal Synthesis of Graphene Nanosheets and Their Polyaniline Nanocomposites for Energy Strorage. *Chem. Mater.* **2009**, 21, (21), 5004-5006.